DOI: 10.1002/chem.201905280

■ Metal–Organic Frameworks

Disappearing Polymorphs in Metal-Organic Framework Chemistry: Unexpected Stabilization of a Layered Polymorph over an Interpenetrated Three-Dimensional Structure in Mercury Imidazolate**

Isaiah R. Speight,^[a] Igor Huskić,^[b] Mihails Arhangelskis,^[b, c] Hatem M. Titi,^[b] Robin S. Stein,^[b] Timothy P. Hanusa,*^[a] and Tomislav Friščić*^[b]

Dedicated to Joel Bernstein (1941–2019) for his contributions to polymorphism of solids and Drago Grdenić (1919–2018) for his work in the chemistry of mercury compounds

Abstract: The "disappearing polymorph" phenomenon is well established in organic solids, and has had a profound effect in pharmaceutical materials science. The first example of this effect in metal-containing systems in general, and in coordination-network solids in particular, is here reported. Specifically, attempts to mechanochemically synthesize a known interpenetrated diamondoid (dia) mercury(II) imidazolate metal-organic framework (MOF) yielded a novel, more stable polymorph based on square-grid (sql) layers. Simultaneously, the dia-form was found to be highly elusive, observed only as a short-lived intermediate in monitoring

solvent-free synthesis and not at all from solution. The destabilization of a dense *dia*-framework relative to a lower dimensionality one is in contrast to the behavior of other imidazolate MOFs, with periodic density functional theory (DFT) calculations showing that it arises from weak interactions, including structure-stabilizing agostic C—H····Hg contacts. While providing a new link between MOFs and crystal engineering of organic solids, these findings highlight a possible role for agostic interactions in directing topology and stability of MOF polymorphs.

Introduction

Metal-organic frameworks (MOFs)^[1] are one of the most active and prolific areas of contemporary materials chemistry, due to their modular design that permits rational incorporation of a diverse range of metal ions and suitably functionalized organic linkers into functional solid-state structures.^[2] Although a significant amount of effort has been invested into developing materials with new and/or improved properties,^[3] fundamental and systematic studies of how the stability and topology of

[a] I. R. Speight, Prof. T. P. Hanusa
Department of Chemistry, Vanderbilt University
Nashville, TN, 37235 (USA)
E-mail: t.hanusa@vanderbilt.edu

[b] Dr. I. Huskić, Dr. M. Arhangelskis, Dr. H. M. Titi, Dr. R. S. Stein, Prof. T. Friščić Department of Chemistry, McGill University Montreal, H3A 0B8 (Canada) E-mail: tomislav.friscic@mcqill.ca

[c] Dr. M. Arhangelskis Faculty of Chemistry, University of Warsaw Warsaw 02-093 (Poland)

[**] A previous version of this manuscript has been deposited on a preprint server (https://doi.org/10.26434/chemrxiv.9725303.v1).

Supporting information and the ORCID identification number(s) for the author(s) of this article can be found under: https://doi.org/10.1002/chem.201905280.

MOFs are affected by component choice and structure have remained less developed. [4,5] Popular MOF designs have mostly focused on lighter main group (e.g., Li, [6] Mg, [7] Al [8]) and firstrow transition metals^[9-13] with the exception of NbOFFIVE, UiOand NU-type MOFs based on Nb, Zr, or Hf.[14-17] Although lanthanide-based systems have been known, including examples of naturally occurring MOFs (e.g., the cerium-based deveroite), [18,19] and recent work has started exploring elements of the 6th period (e.g. Th, U, Np) as nodes, the properties and formation of MOFs with heavier members of the periodic table remain poorly explored. [20-22] Consequently, it is unknown to what extent such heavy elements are compatible with, and can bring novelty to, MOF designs. This is particularly relevant for topologically flexible MOFs, a case in point being zeolitic imidazolate frameworks (ZIFs)[23] and other azolates,[24] that are prone to polymorphism and will adopt a wide range of topologies depending on metal and linker choice. [25] Although it is well known that such networks can adopt different topologies depending on inclusion of solvent guests, the behavior of true framework polymorphs, that is, structurally different materials of identical chemical composition in which there are no included guests, remains a poorly explored area of MOF chemistry that has only recently sparked the interest of the research community.[26,27] Although the most popular ZIFs (e.g., sodalite-topology ZIF-8, ZIF-67) are based on open, microporous



structures, our group and others have shown that their behavior reflects that of inorganic tetrahedral solids,^[5,28] with thermodynamically stable true polymorphs of such materials being dense, sometimes interpenetrated, three-dimensional (3D) frameworks of *zni-*, *dia-* or *qtz*-topology.^[25–27]

We report here the unusual destabilization of such an interpenetrated, dense *dia*-topology ZIF (Figure 1a) relative to a layered structure based on two-dimensional (2D) *sql*-sheets, in a mercury(II) imidazolate framework. Stabilization of the 2D

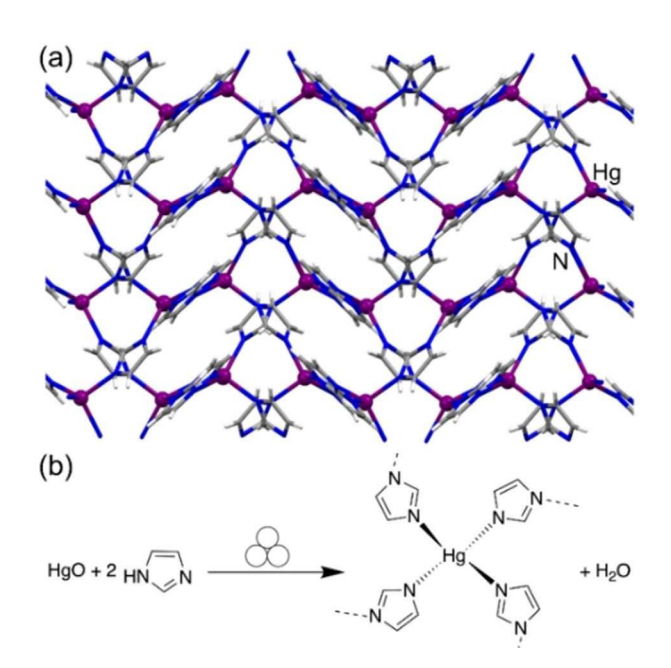


Figure 1. (a) View of the previously reported⁽³³⁾ crystal structure (CSD code BAYPUN) of interpenetrated dia-Hg(lm) $_2$ and (b) the herein explored mechanochemical reaction. The symbol for mechanochemical reaction conditions is adopted from Ref. [35].

structure is due to weak interactions that include short C-H...Hg contacts, providing a unique example of intermolecular agostic interactions contributing to thermodynamic selection of a MOF structure. Although the herein reported new sqlpolymorph of mercury(II) imidazolate is readily obtained using different solution and solid-state techniques, the originally reported dia-topology was almost impossible to reproduce, except as a fleeting intermediate phase. The difficulty of obtaining a previously reported crystalline phase has been well documented in crystal engineering of organic molecular solids as the "disappearing polymorph" phenomenon, which is explained by the metastable nature of the first reported polymorph with respect to a subsequently observed, thermodynamically more stable, phase. As this phenomenon has to date been observed only in discrete molecular organic solids, [29,30] the herein presented work represents, to the best of our knowledge, the first documented example of the disappearing polymorph phenomenon not only in MOFs, but also in the broader context of coordination compounds and network solids.[29,30]

Mercury (as Hg²⁺) is attractive for investigating the effect of heavy elements on ZIF chemistry, as it is the heaviest accessi-

ble homologue of Zn²⁺, the most extensively used node in ZIF design. [22-27] As ZIFs with Cd²⁺ have also been studied, [31] using Hg²⁺ as a node offers a unique opportunity to explore MOF formation across an entire series of homologous transition metals.[32] To date, there has been only one report of a mercury-based imidazolate framework, the dia-topology mercury(II) imidazolate Hg(Im)₂.^[33,34] The framework (CSD code BAYPUN) was reported to be isostructural to its cadmium analogue dia-Cd(Im)₂ that represents the dense, stable polymorph among several known Cd(Im)₂ structures.^[31] Both dia-Cd(Im)₂ and -Hg(Im)₂ were first reported in 2003 to be formed by precipitation from aqueous solution, and were structurally characterized from powder X-ray diffraction (PXRD) data by Masciocchi et al. (Figure 1 a).[33] In 2006, Fernández-Bertrán et al. attempted the synthesis of Hg(Im)₂ mechanochemically,^[35,36] and established that manual grinding of HgO and imidazole (Hlm) led to partial formation of a material with hexagonal symmetry, distinct from dia-Hg(Im)2.

Results and Discussion

Intrigued by the apparent difference in mechanochemical and solution-based routes to $Hg(Im)_2$, we re-investigated the mechanochemical reaction by ball milling HgO and HIm in the respective 1:2 stoichiometric ratio (Figure 1b), a methodology previously shown to be highly successful in making zinc ZIFs. [25] Milling was performed in a 25 mL Teflon jar by using one ZrO_2 ball (3.25 g, see Supporting Information). Chemical reaction upon milling was evident by a change in color of the reaction mixture from orange (due to HgO) to colorless. After 30 min milling, PXRD analysis revealed the total absence of Bragg reflections of reactants, indicating complete conversion (Figure 2a). Unexpectedly, the product exhibited X-ray reflec-

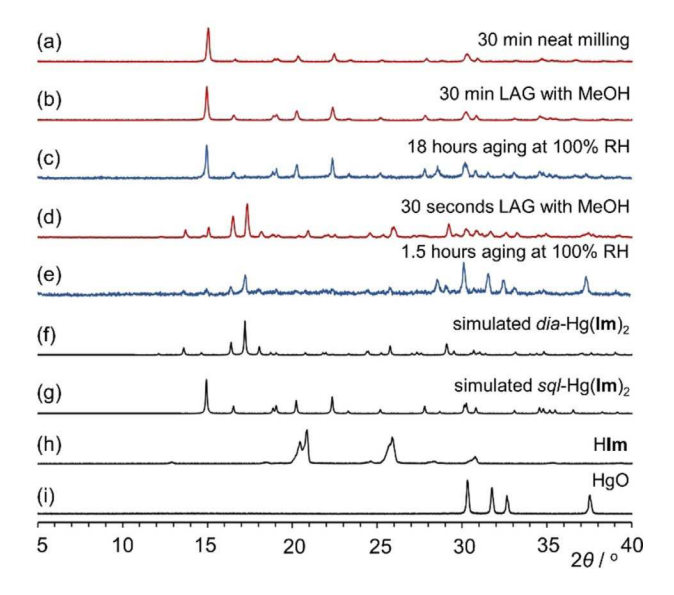


Figure 2. Comparison of selected PXRD patterns for the reactions of HgO and H**Im**: (a) after 30 min neat milling; (b) after 30 min LAG with MeOH; (c) after 18 h aging at 100% RH; (d) after 30 sec LAG with MeOH; (e) after 1.5 h aging at 100% RH; (f) simulated for *dia*-Hg(**Im**)₂ (CSD BAYPUN); (g) simulated for *sql*-Hg(**Im**)₂ and measured for: (h) H**Im**; (i) HgO.



tions that did not match either the dia-Hg(\mathbf{Im})₂ structure or the product of Fernández-Bertrán et al. [36]

The reaction was repeated with liquid-assisted grinding (LAG), [37] a method in which the reaction progress is accelerated and directed by small amounts of a liquid. The outcome of the mechanochemical reaction did not change upon LAG with different liquids, including methanol (MeOH, Figure 2b), N,N-dimethylformamide (DMF), acetonitrile (MeCN), or water (see Supporting Information). Moreover, attempts to prepare the known $\mathit{dia}\text{-Hg}(\mathbf{Im})_2$ by following the reported [33] solution synthesis were unsuccessful, yielding a microcrystalline powder with a PXRD pattern identical to that of the material made by milling. Thermogravimetric analysis (TGA) of the product revealed no weight loss until the decomposition temperature of about 200 °C, indicating that the material does not contain guest solvent. Comparison of the samples prepared mechanochemically and from solution with scanning electron microscopy (SEM) revealed particles of similar block-shaped morphology. However, different methods of preparation led to differences in particle sizes: mechanochemically made material exhibited particles with sizes of approximately 200-1000 nm, whereas solution-made material consisted of elongated blocks mostly in the 10–20 μm range (see Supporting Information).

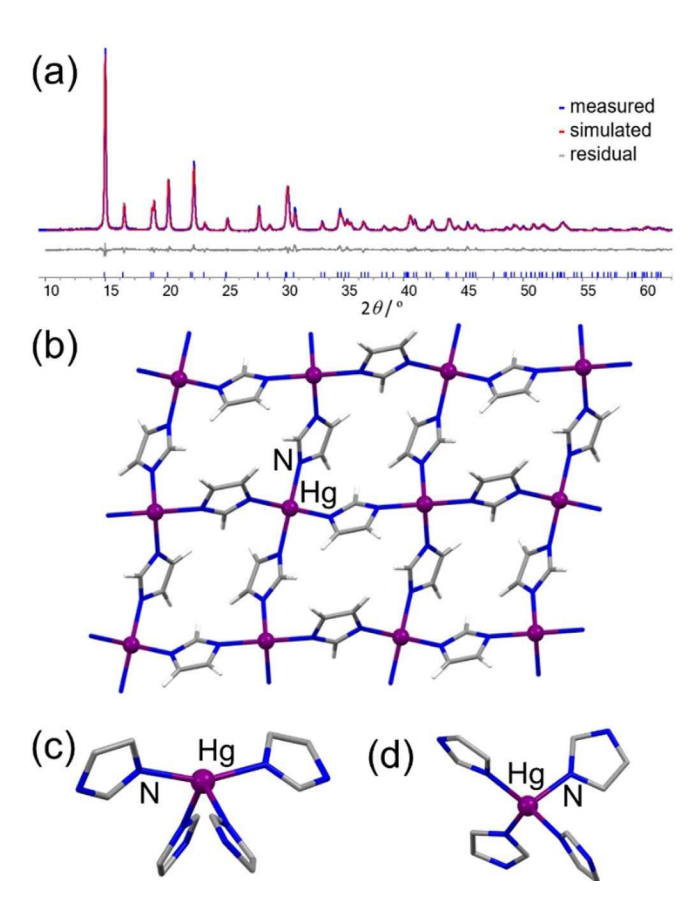


Figure 3. (a) Final Rietveld refinement fit for the structure of sql-Hg(lm)₂: the experimental PXRD pattern is shown in blue, the calculated pattern in red, and the difference curve in grey. (b) View of a single layer of sql-Hg(lm)₂ along the crystallographic c-axis. Comparison of the coordination geometries of the metal node in: (c) sql-Hg(lm)₂ and (d) dia-Hg(lm)₂, with hydrogen atoms omitted for clarity.

The PXRD pattern of mechanochemically prepared material was readily indexed to an orthorhombic unit cell in the space group $P2_12_12$, with a=9.4089(4) Å, b=7.6414(3) Å, c=5.3625(2) Å, and V=385.55(3) Å³. Structure solution and Rietveld refinement revealed a polymorph of $Hg(\mathbf{Im})_2$ based on two-dimensional (2D) sheets with a square-grid (sqI) topology (Figure 3 a,b).

In contrast to the previously reported dia-Hg(\mathbf{Im})₂, in which Hg²⁺ adopts a roughly tetrahedral coordination with N-Hg-N angles in the range of 98.3–117.7° and Hg–N bonds in the range of 2.18–2.32 Å, the geometry of Hg²⁺ in sql-Hg(\mathbf{Im})₂ is highly distorted, best described as "see-saw" (Figure 3 c). Specifically, the environment of each Hg²⁺ is defined by two shorter [2.18(2) Å] Hg–N bonds at an angle of 156.1(6)°, and a pair of longer ones [2.31(2) Å], at an angle of 104.6(7)° (Figure 3 d).

The geometry can be described more quantifiably by means of the $\tau_{4}^{\,[38]}$ and $\tau_{4}^{\,'[39]}$ structural parameters, which are derived from metal-centered bond angles. Values of τ_4 close to 1 imply a tetrahedral geometry, those close to 0 a square planar arrangement, and intermediate values are associated with various sawhorse structures. For the sql-Hg(\mathbf{Im})₂ structure, $\tau_4 = 0.60$ and $\tau_4' = 0.28$. This value of τ_4 corresponds to a sawhorse geometry, slightly distorted toward a tetrahedral configuration. In this case, the low value of τ_4 indicates that the effective coordination number of the metal may actually be higher than 4, a situation first noticed in a complex with Hg $\cdot\cdot\cdot\pi$ interactions. [40] In the present case, additional short H.-.Hg contacts, described in more detail below, appear to fulfill this role. In contrast to other reported sql-topology ZIFs, Ni(Im), (CSD ALIDUU)[41] and zinc benzimidazolate (CSD KOLYAM),[42] where neighboring layers arrange in an offset way, the sheets in sql-Hg(Im)₂ stack

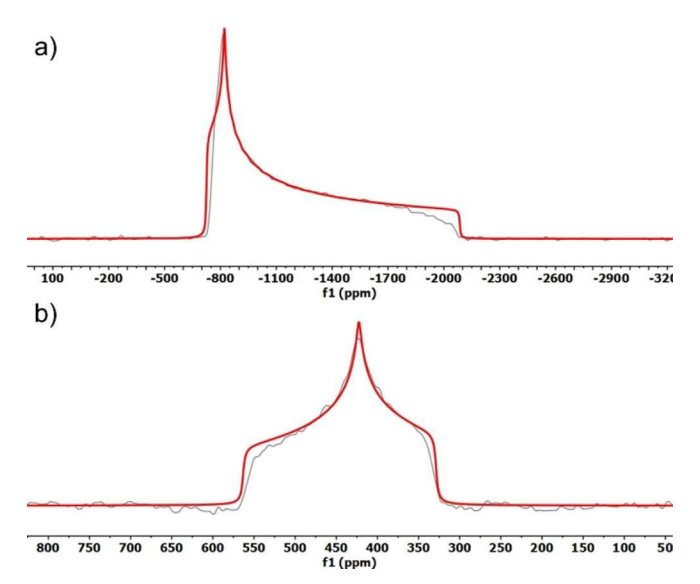


Figure 4. a) Overlay of the fit (red) to the static solid-state $^{199}\mathrm{Hg}$ NMR powder pattern of $sql\text{-Hg}(\mathbf{Im})_2$ (grey). The pattern shows that the chemical shift tensor at the mercury nucleus has nearly axial symmetry (isotropic chemical shift $\delta_{\mathrm{iso}} = -1212.5$ ppm, span $\Omega = 1366$ ppm, skew $\kappa = 0.9$); b) overlay of the fit (red) to the static solid-state $^{113}\mathrm{Cd}$ NMR powder pattern of $dia\text{-Cd}(\mathbf{Im})_2$ (grey). The pattern shows non-axial chemical shift anisotropy (isotropic chemical shift $\delta_{\mathrm{iso}} = 438.2$ ppm, span $\Omega = 235.0$ ppm, skew $\kappa = -0.2$).

directly on top of each other (see Supporting Information). The coordination of $\mathrm{Hg^{2+}}$ in $\mathit{sql}\text{-}\mathrm{Hg}(\mathrm{Im})_2$ is consistent with its axially symmetric ¹⁹⁹Hg solid-state nuclear magnetic resonance (ssNMR) powder pattern (Figure 4a),^[43] very different from the anisotropic ¹¹³Cd pattern observed in $\mathit{dia}\text{-}\mathrm{Cd}(\mathrm{Im})_2$ (Figure 4b) and would have been expected also for the ¹⁹⁹Hg spectrum of isostructural $\mathit{dia}\text{-}\mathrm{Hg}(\mathrm{Im})_2$.

We were surprised that all explored mechanochemical and solution-based experiments yielded only sql-Hg(Im)2, without any evidence of the previously reported polymorph dia-Hg(Im)₂, or the hexagonal phase reported by Fernández-Bertrán. [36] Moreover, thermal analysis of sql-Hg(Im)2, including differential scanning calorimetry, thermogravimetric analysis and variable-temperature PXRD all confirmed that the material retained its structure until chemical decomposition at about 200 °C (see Supporting Information). In contrast to unsuccessful attempts to synthesize dia-Hg(Im)2, we readily reproduced the dense phase of zinc imidazolate (zni-Zn(Im)2) and the dense dia-Cd(Im), phase reported by Masciocchi et al. [33] and others, [29] using either mechanochemical or solution synthesis (see Supporting Information). In an attempt to reproduce any of the reported Hg(Im)₂ phases, we explored a milder synthetic route, by aging^[44] a 1:2 stoichiometric mixture of HgO and HIm at 100% relative humidity. Real-time PXRD monitoring^[45] (Figure 5 a) revealed X-ray reflections of dia-Hg(Im), (Figure 2 e,c), and Rietveld analysis of the in situ data revealed that the content of dia-Hg(Im)2 increases for approximately 90 min, after which it diminishes and sql-Hg(Im)₂ appears (Figure 5b). After 140 min, the PXRD pattern exhibits only sql-Hg(Im)₂. The initial, short-lived appearance of dia-Hg(Im), in aging led us to explore the milling reaction of HgO and HIm at short reaction times. Indeed, PXRD analysis after 30 seconds LAG with MeOH revealed the appearance of dia-Hg(lm) $_2$ along with unreacted HgO and HIm (Figure 2d). After 1 min, the reaction mixture exhibits only reflections of sql-Hg(lm)₂.

The difficulty in reproducing the previously reported dia-Hg(Im)₂ phase resembles the disappearing polymorph^[29,30] phenomenon reported in molecular organic crystalline solids, in which a first-reported polymorph is subsequently found to be metastable and difficult to reproduce compared to a later obtained, and usually more stable, polymorph. However, such behavior has not yet been reported for metal-containing systems with either molecular or network structures. So far, investigations of phase landscapes for ZIFs based on four-coordinate metal atoms have shown resemblance to zeolites and other tetrahedral structures, with the phases of greater density being the more stable ones. For dia- and sql-Hq(Im), the relative stabilities are not readily deduced from their calculated densities, which are very similar: 2.87 and 2.88 g cm⁻³, respectively. However, the difficulty in synthesizing the dia-phase, and the dia→sql transformation seen in aging and milling, indicates that the sql-form should be the thermodynamically more stable phase in the Hg(Im)₂ system.^[25] This was supported by slurry shaking experiments, as there were no changes in sample PXRD patterns upon shaking of sql-Hg(Im)2 in either water or common organic solvents (MeOH, ethanol, CH₃CN, CHCl₃, acetone) over two days (see Supporting Information).

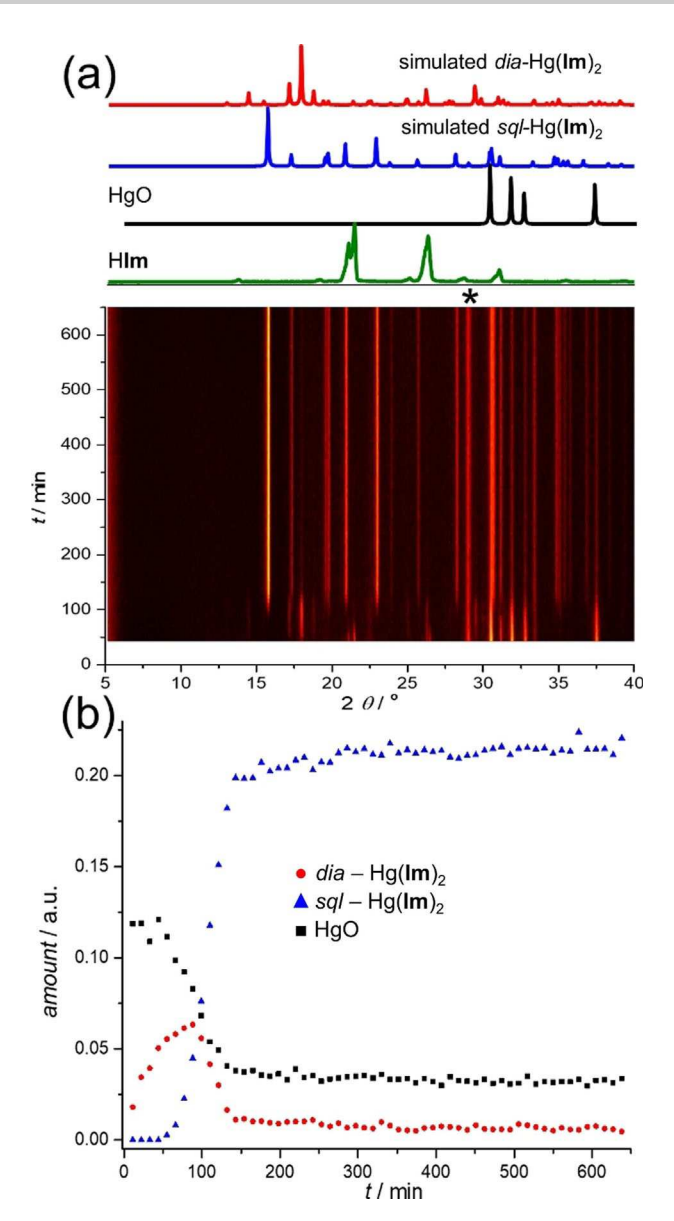


Figure 5. Real-time monitoring of the aging reaction of HgO and Hlm by PXRD: (a) time-resolved diffractogram, with diffraction patterns of selected phases shown on top, and Bragg reflection of CeO₂ standard labeled with "*"; (b) reaction profile based on Rietveld fitting, demonstrating changes in amount of HgO, *dia*- and *sql*-Hg(lm)₂. Quantitative kinetics analysis was hindered by preferred orientation in the static reaction mixture.

The stability of sql-Hg(\mathbf{Im})₂ was also validated by periodic density functional theory (DFT) calculations, performed with the periodic DFT code CRYSTAL17^[46] using the hybrid B3LYP^[47] functional combined with the Grimme D3 semiempirical dispersion correction, which showed that the sql-form is 10.21 kJ mol⁻¹ lower in energy than the dia-one. This contrasts with $Zn(\mathbf{Im})_2^{[49]}$ and $Zd(\mathbf{Im})_2$, the most stable forms of which exhibit three-dimensional (3D) Zni- and Zni- and



sql-Hg(lm)₂ with cadmium. In this case, the two structures were found to have essentially indistinguishable energies, with sql-Cd(lm)₂ being just 0.39 kJ mol⁻¹ more stable. The improved stability of the dia-structure in Cd(lm)₂ is consistent with the herein confirmed experimental reproducibility (see Supporting Information) and multiple previous observations of dia-Cd(lm)₂. [31]

Stabilization of the 2D sql-structure in $Hg(\mathbf{Im})_2$, compared to a more extensively connected, interpenetrated 3D dia-framework, is unexpected and, we believe, associated with weak interactions between layers. This view is supported by calculations of the relative stabilities of dia- and sql- $Hg(\mathbf{Im})_2$ using the B3LYP functional uncorrected for dispersion. Under such conditions, which artificially ignore the contributions of van der Waals interactions, the stabilities of the two structures become inverted, with the dia-form becoming 7.81 kJ mol $^{-1}$ more stable.

Whereas the sql-Hg(Im)₂ structure reveals short contacts between neighboring layers, readily interpreted as C–H $\cdots\pi$ and $\pi \cdots \pi$ interactions, it also exhibits short H···Hg contacts at 3.26(3) Å, not present in the dia-form. Each Hg atom participates in two such contacts with symmetry-related imidazolate groups (Figure 6). Most proposed van der Waals radii for Hg range from 2.00 to 2.53 Å, [50] indicating that these contacts might be roughly 10% shorter than the sum of van der Waals radii of H (1.20 Å) and Hg. The shortness of these contacts lends itself to two possible explanations. The contacts can be interpreted either as hydrogen-bonding interactions of the C-H···Hg type, where the σ^* -orbital C–H moiety is interacting with available electron density on the metal atom, or a C-H...Hg agostic interaction, [51] where the empty orbitals on the metal ion are associated with the σ -electron density of the C-H bond. [52,53] Of these two interpretations, the formation of

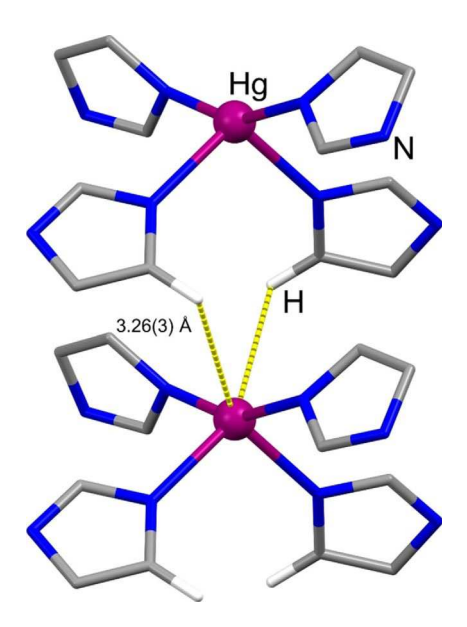


Figure 6. Fragment of the crystal structure of *sql*-Hg(**Im**)₂ illustrating the short H···Hg contacts between neighboring metal–organic layers. Hydrogen atoms, except the ones relevant for illustrating the H···Hg contacts, have been omitted for clarity.

weak agostic bonds is the more likely one, as the metal node is expected to be electron-poor in the +2 oxidation state, and associated with four electronegative azolate ligands.

To better understand the nature of C-H...Hg interactions as well as the unique appearance and energetic stability of sql-Hg(Im)₂, as opposed to its hypothetical sql-Cd(Im)₂ analogue, we performed Bader's quantum theory of atoms in molecules (QTAIM)[54,55] analysis on the DFT-optimized structures. Specifically, we searched for bond critical points (BCPs) as evidence for structure-stabilizing interactions. The experimental sql-Hg(Im)₂ structure and the computationally generated isostructural sql-Cd(Im)₂ structure display a very similar distribution of non-covalent BCPs (Figure 7, also see Supporting Information), with the exception of one BCP in the vicinity of the Hg atom (Figure 7a). This critical point, which is the highest in the sql-Hg(Im)₂ structure, reveals a moderate bonding interaction (0.074 electrons $Å^{-3}$) between the C-H group and the Hg atom in neighboring layers (Figure 7a, b, see also Supporting Information). This BCP coincides with the experimentally noted short H...Hg contact between layers and, importantly, it is re-

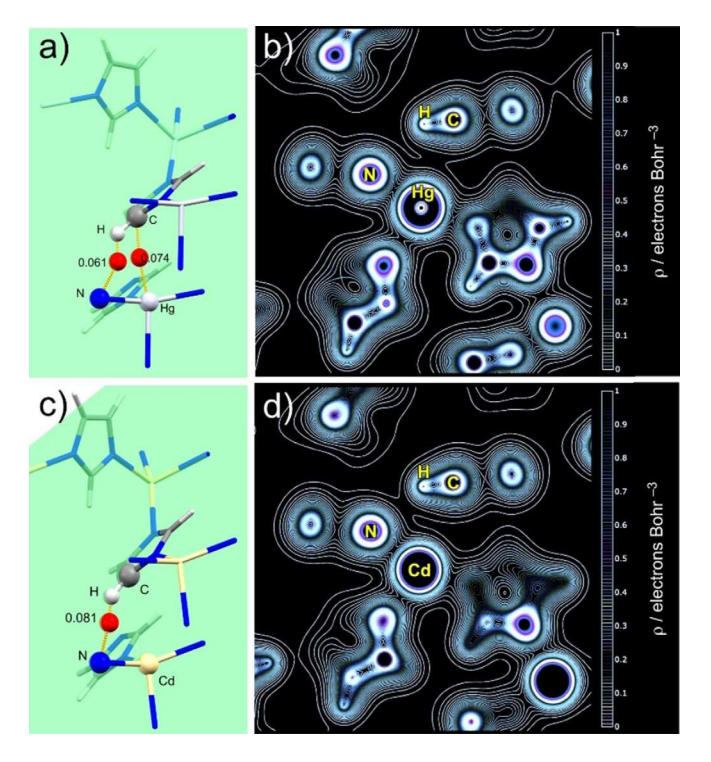


Figure 7. The highest bond critical points (BCPs) for the experimental sql-Hg(lm) $_2$ (top) and theoretically generated sql-Cd(lm) $_2$ (bottom) structures: a) structure plot showing a C–H···Hg bonding interaction with a BCP with electron density (ρ) of 0.074 electrons Å⁻³ and a C–H···N bonding interaction with a BCP with ρ of 0.061 electrons Å⁻³ in sql-Hg(lm) $_2$; b) 2D contour plot showing the electron density distribution in sql-Hg(lm) $_2$; c) Structure plot showing a C–H···N bonding interaction with a BCP with ρ of 0.081 electrons Å⁻³ in sql-Cd(lm) $_2$; d) 2D contour plot showing the electron density distribution in sql-Cd(lm) $_2$. In all cases the green plane shows the orientation of the contour plot slices. The plots indicate that the dominant interaction between the 2D layers of sql-Hg(lm) $_2$ framework occurs sidewise between the C–H group and the metal atom, consistent with an agostic contact involving the σ-orbital of the hydrocarbon moiety. This contrasts the hypothetical analogous structure based on cadmium (see Supporting Information), in which the dominant interaction would be a C–H···N hydrogen bond.

5



tained regardless of whether the dispersion correction is applied in structure optimization or not. The second highest BCP in the *sql*-Hg(**Im**)₂ structure is also located near the metal atom, but clearly represents a stabilizing C—H···N hydrogen-bonding interaction.

The electron density analysis is different for the putative sql-Cd(\mathbf{Im})₂ structure, which does not exhibit any BCPs involving the metal center. Instead, the highest BCP in the sql-Cd(\mathbf{Im})₂ structure overlaps with the second-highest BCP of sql-Hg(\mathbf{Im})₂ and corresponds to a stabilizing C–H···N hydrogen-bonding interaction between the metal–organic sheets (Figure 7 c,d, see also Supporting Information).

The Bader analysis shows that the short H···Hg contacts in sql-Hq(Im), are clearly of a stabilizing nature, and the positioning of their corresponding BCPs indicates a "side-on" interaction of the hydrocarbon moiety and the Hg atom, which is consistent with the participation of the C–H bond σ -electron density. Finally, the pair of short C-H---Hg contacts in sql-Hg(Im)₂ can be interpreted as completing the unusual see-saw geometry, established by nitrogen azolate ligands, into a distorted octahedron. All of these observations are consistent^[52] with the appearance of weak C-H···Hg agostic bonds^[51,52,55,56] between metal-organic layers that contribute to the overall stabilization of the sql-Hg(Im)2 structure. As BCPs corresponding to such stabilizing contacts do not appear in the hypothetical sql-Cd(Im)₂ structure, they also provide a possible explanation for the difference in structural preferences of dense phases of mercury(II) and cadmium(II) imidazolates.

Conclusions

In summary, a re-investigation of an early report of mechanochemical MOF formation has revealed a novel, layered polymorph of a unique mercury(II) imidazolate framework. Experiment and theory indicate that the layered polymorph is thermodynamically more stable than the previously reported interpenetrated dia-framework, evidently due to weak intermolecular forces that include interlayer agostic C-H---Hg contacts. At the same time, we were unable to obtain the originally reported dia-structure in pure form and have observed it only as a fleeting intermediate during solid-state synthesis, sometimes not lasting more than a minute. The difficulty in reproducing the dia-polymorph makes mercury(II) imidazolate, to the best of our knowledge, the first documented example of the disappearing polymorph phenomenon in coordination chemistry. This new parallel with crystal engineering of organic solids^[57] is of high relevance for the ongoing commercialization of MOFs. [58] By analogy with organic pharmaceutical solids, [30] for which polymorphism and problems of phase nucleation^[59] are recognized as major challenges in their development and industrial manufacture, the discovery of the disappearing polymorph phenomenon in coordination networks is of relevance in the commercial development of MOFs, as some of the previously reported materials might prove difficult to reproduce.

The demonstrated stabilization of a layered structure marks a striking contrast between Hg^{2+} and its congeners Cd^{2+} and Zn^{2+} , the imidazolates of which in their most stable form favor

3D frameworks, highlighting the potential for differences in MOF formation when using a heavy element compared to its lighter congeners, and suggesting a possible role for even weak agostic interactions^[51–55] in directing polymorphism in MOF structures. We believe that the results of this work are of significance for understanding the formation of layered MOFs, which have recently become of considerable interest as functional materials,^[60] and are pursuing further studies of systems based on heavy elements.

Experimental Section

Experimental Details: The herein provided information is a general overview of selected procedures only. More extensive descriptions and data on experimental and computational procedures, structure analysis, as well as selected X-ray diffraction, infrared and solid-state NMR spectroscopy data are provided in the Supplementary Information file.

Crystallographic data: CCDC 1948341 sql-Hg(lm) $_2$ contains the supplementary crystallographic data for this paper. These data can be obtained free of charge from The Cambridge Crystallographic Data Centre.

General information: HgO (≥99%) and imidazole (HIm) (≥99%) were purchased from Aldrich. Methanol (MeOH), N,N-dimethylformamide (DMF), and acetonitrile (MeCN) were purchased from ACP Chemicals. All chemicals were used without further purification. Mercury compounds should be treated with rigorous safety precautions due to their toxicity. Care was taken at all times to avoid contact with solid, solution, and air-borne particulate mercury compounds. All reactions, equipment, and waste were treated and disposed of properly.

Mechanochemical experiments: Reactions were conducted in a Teflon milling jar of 25 mL volume, using one 7 mm diameter (weight $\approx 3.2\,\mathrm{g}$) zirconia ball, and either a Retsch MM400 or Retsch MM200 mill operating at 25 Hz. In a typical experiment, a solid mixture of HgO (108.3 mg, 0.50 mmol) and Hlm (68.1 mg, 1.00 mmol, 1:2 stoichiometric ratio with respect to total mercury content) was placed in a 25 mL Teflon jar along with either 50 μL of MeOH, MeCN, DMF, water, or no additive, and the reaction mixture was milled for a period of 30 min. The material was analyzed without further treatment.

Synthesis of sql-**Hg(Im)** $_2$ **from solution**: A 250 mL round bottom flask was charged with a Teflon stirring bar, mercury(II) acetate (5.00 g, 15.7 mmol, 1 equiv), and HIm (4.25 g, 62.4 mmol, 4 equiv). Next, 100 mL of de-ionized water was added to the flask and the solution was stirred. Aqueous ammonia (28% v/v) (7.01 mL, 68.1 mmol) was added slowly down the side of the flask. The reaction was allowed to stir at ambient temperature for 3 h. The reaction was then filtered and the isolated material was washed twice with 25 mL portions of de-ionized water, washed once with 25 mL of methanol and then dried.

Reactions by aging: Samples of HgO (108.3 mg, 0.50 mmol, 1 equiv) and H**Im** (68.1 mg, 1 mmol, 2 equiv) were ground separately in a mortar and pestle. The two solids were placed in a vial along with CeO_2 (17.6 mg, 10% w/w) as an internal X-ray diffraction standard. The mixture was agitated in a vial to create a homogenous mixture. A small portion of the mixture was then transferred to a custom designed PXRD sample holder^[42] with two grooves ground into the surface. In each groove was placed 200 μ L of water to act as a source of humidity. The holder was covered with a small sheet of Saran wrap to seal the chamber and

6



generate a saturated humidity atmosphere. Samples were aged under this atmosphere for 17.5 h, with PXRD patterns recorded periodically every 11.4 min.

Acknowledgements

I.R.S. and T.P.H. acknowledge financial support by the NSF (CHE-1665327) and ACS-PRF (56027-ND3); TF acknowledges support of NSERC (RGPIN-2017-06467, STPGP 521582-18). MA acknowledges support of NCN (2018/31/D/ST5/03619). We thank Prof. R. W. Schurko (National MagLab) and Dr. V. Zorin (JEOL) for help setting up the BRAIN-CP/WURST-CPMG pulse sequences.

Conflict of interest

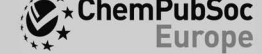
The authors declare no conflict of interest.

Keywords: mechanochemistry · mercury · metal-organic frameworks · polymorph · solid state

- [1] S. R. Batten, N. R. Champness, X.-M. Chen, J. Garcia-Martinez, S. Kitagawa, L. Öhrstrom, M. O'Keeffe, M. Paik Suh, J. Reedijk, CrystEngComm **2012**. 14. 3001 - 3004.
- [2] a) B. Rungtaweevoranit, C. S. Diercks, M. J. Kalmutzki, O. M. Yaghi, Faraday Discuss. 2017, 201, 9-45; b) P. Deria, J. E. Mondloch, O. Karagiaridi, W. Bury, J. T. Hupp, O. K. Farha, Chem. Soc. Rev. 2014, 43, 5896-5912.
- [3] a) H. Furukawa, N. Ko, Y. B. Go, N. Aratani, S. B. Choi, E. Choi, A. Ö. Yazaydin, R. Q. Snurr, M. O'Keeffe, J. Kim, O. M. Yaghi, Science 2010, 329, 424-428; b) M. F. de Lange, K. J. F. M. Verouden, T. J. H. Vlugt, J. Gascon, F. Kapteijn, Chem. Rev. 2015, 115, 12205 - 12250; c) A. J. Tansell, C. L. Jones, T. L. Easun, Chem. Cent. J. 2017, 11, 100; d) F.-X. Coudert, Chem. Mater. 2015, 27, 1905 - 1916.
- [4] a) M. E. Schweinefuß, S. Springer, I. A. Baburin, T. Hikov, K. Huber, S. Leoni, M. Wiebcke, Dalton Trans. 2014, 43, 3528-3536; b) F.-X. Coudert, A. H. Fuchs, Coord. Chem. Rev. 2016, 307, 211-236; c) T. L. Easun, F. Moreau, Y. Yan, S. Yang, M. Schröder, Chem. Soc. Rev. 2017, 46, 239-
- [5] a) M. Arhangelskis, A. D. Katsenis, A. J. Morris, T. Friščić, Chem. Sci. 2018, 9, 3367-3375; b) H. M. Titi, M. Arhangelskis, A. D. Katsenis, C. Mottillo, G. Ayoub, J.-L. Do, A. M. Fidelli, R. D. Rogers, T. Friščić, Chem. Mater. **2019**, *31*, 4882 – 4888.
- [6] J. Zhang, T. Wu, C. Zhou, S. Chen, P. Feng, X. Bu, Angew. Chem. Int. Ed. **2009**, 48, 2542–2545; Angew. Chem. **2009**, 121, 2580–2583.
- [7] D. Gygi, E. D. Bloch, J. A. Mason, M. R. Hudson, M. I. Gonzalez, R. L. Siegelman, T. A. Darwish, W. L. Queen, C. M. Brown, J. R. Long, Chem. Mater. 2016, 28, 1128 - 1138.
- [8] T. Loiseau, C. Serre, C. Huguenard, G. Fink, F. Taulelle, M. Henry, H. Bataille, G. Férey, Chem. Eur. J. 2004, 10, 1373 - 1382.
- [9] G. Ferey, C. Mellot-Draznieks, C. Serre, F. Millange, J. Dutour, S. Surblé, I. Margiolaki, Science 2005, 309, 2040 - 2042.
- [10] J. López-Cabrelles, J. Romero, G. Abellán, M. Giménez-Marqués, M. Polomino, S. Valencia, F. Rey, G. Mínguez Espallargas, J. Am. Chem. Soc. **2019**, 141, 7173 - 7180.
- [11] H. Deng, S. Grunder, K. E. Cordova, C. Valente, H. Furukawa, M. Hmadeh, F. Gándara, A. C. Whalley, Z. Liu, S. Asahina, H. Kazumori, M. O'Keeffe, O. Terasaki, J. F. Stoddart, O. M. Yaghi, Science 2012, 336, 1018-1023.
- [12] G. Zhong, D. Liu, J. Zhang, J. Mater. Chem. A 2018, 6, 1887 1899.
- [13] S. S.-Y. Chui, S. M.-F. Lo, J. P. H. Charmant, A. G. Orpen, I. D. Williams, Science 1999, 283, 1148-1150.
- [14] P. M. Bhatt, Y. Belmabkhout, A. Cadiau, K. Adil, O. Shekhah, A. Shkurenko, L. J. Barbour, M. Eddaoudi, J. Am. Chem. Soc. 2016, 138, 9301-9307.
- [15] J. Hafizovic-Cavka, S. Jakobsen, U. Olsbye, N. Guillou, C. Lamberti, S. Bordiga, K. P. Lillerud, J. Am. Chem. Soc. 2008, 130, 13850-13851.

- [16] T. C. Wang, N. A. Vermeulen, I. S. Kim, A. B. F. Martinson, J. F. Stoddart, J. T. Hupp, O. K. Farha, Nat. Protoc. 2016, 11, 149 – 162.
- [17] M. J. Cliffe, W. Wan, X. Zou, P. A. Chater, A. K. Kleppe, M. G. Tucker, H. Wilhelm, N. P. Funnell, F.-X. Coudert, A. L. Goodwin, Nat. Commun. 2014,
- [18] M. Lammert, M. T. Wharmby, S. Smolders, B. Bueken, A. Lieb, K. A. Lomachenko, D. De Vos, N. Stock, Chem. Commun. 2015, 51, 12578-12581.
- [19] a) I. Huskić, T. Friščić, Acta Crystallogr. Sect. B 2018, 74, 539-559; b) T. Devic, C. Serre, N. Audebrand, J. Marrot, G. Férey, J. Am. Chem. Soc. 2005, 127, 12788 – 12789; c) X. Guo, G. Zhu, Z. Li, F. Sun, Z. Yang, S. Qiu, Chem. Commun. 2006, 3172-3174.
- [20] a) K. P. Carter, J. A. Ridenour, M. Kalaj, C. L. Cahill, Chem. Eur. J. 2019, 25, 7114-7118; b) E. A. Dolgopolova, A. M. Rice, N. B. Shustova, Chem. Commun. 2018, 54, 6472-6483.
- [21] a) C. Falaise, C. Volkringer, J.-F. Vigier, N. Henry, A. Beaurain, T. Loiseau, Chem. Eur. J. 2013, 19, 5324-5331; b) S. E. Gilson, P. Li, J. E. S. Szymanowski, J. White, D. Ray, L. Gagliardi, O. K. Farha, P. C. Burns, J. Am. Chem. Soc. 2019, 141, 11842-11846.
- [22] a) Y. Zhang, B. E. G. Lucier, S. M. McKenzie, M. Arhangelskis, A. J. Morris, T. Friščić, J. W. Reid, V. V. Terskikh, M. Chen, Y. Huang, ACS Appl. Mater. Interfaces 2018, 10, 28582-28596; b) L. Robison, L. Zhang, R. J. Drout, P. Li, C. R. Haney, A. Brikha, H. Noh, B. L. Mehdi, N. D. Browning, V. P. Dravid, Q. Cui, T. Islamoglu, O. K. Farha, ACS Appl. Biomat. 2019, 2, 1197-1203.
- [23] K. S. Park, Z. Ni, A. P. Côte, J. Y. Choi, R. Huang, F. J. Uribe-Romo, H. K. Chae, M. O'Keeffe, O. M. Yaghi, Proc. Natl. Acad. Sci. USA 2006, 103, 10186-10191.
- [24] J.-P. Zhang, Y.-B. Zhang, J.-B. Lin, X.-M. Chen, Chem. Rev. 2012, 112, 1001 - 1033.
- [25] a) Z. Akimbekov, A. D. Katsenis, G. P. Nagabushana, G. Ayoub, M. Arhangelskis, A. J. Morris, T. Friščić, A. Navrotsky, J. Am. Chem. Soc. 2017, 139, 7952 – 7957; b) P. J. Beldon, L. Fábián, R. S. Stein, A. Thirumurugan, A. K. Cheetham, T. Friščić, Angew. Chem. Int. Ed. 2010, 49, 9640 - 9643; Angew. Chem. 2010, 122, 9834-9837.
- [26] a) R. Galvelis, B. Slater, A. K. Cheetham, C. Mellot-Draznieks, CrystEng-Comm 2012, 14, 374-378; b) D. W. Lewis, A. R. Ruiz-Salvador, A. Gómez, L. M. Rodriguez-Albelo, F.-X. Coudert, B. Slater, A. K. Cheetham, C. Mellot-Draznieks, CrystEngComm 2009, 11, 2272 - 2276; c) C. A. Schröder, I. A. Baburin, L. van Müllen, M. Wiebcke, S. Leoni, CrystEngComm 2013, 15, 4036-4040; d) J. T. Hughes, T. D. Bennett, A. K. Cheetham, A. Navrotsky, J. Am. Chem. Soc. 2013, 135, 598-601; e) A. W. Thornton, K. E. Jelfs, K. Konstas, C. M. Doherty, A. J. Hill, A. K. Cheetham, T. D. Bennett, Chem. Commun. 2016, 52, 3750-3753.
- [27] a) M. Arhangelskis, A. D. Katsenis, N. Novendra, Z. Akimbekov, D. Gandrath, J. M. Marrett, G. Ayoub, A. J. Morris, O. K. Farha, T. Friščić, A. Navrotsky, J. Chem. Mater. 2019, 31, 3777-3783; b) P. F. Rosen, J. J. Calvin, M. S. Dickson, A. D. Katsenis, T. Friščić, A. Navrotsky, N. L. Ross, A. I. Kolesnikov, B. F. Woodfield, J. Chem. Thermodyn. 2019, 136, 160-169; c) J. J. Calvin, M. Asplund, Z. Amirbekov, G. Ayoub, A. D. Katsenis, A. Navrotsky, T. Friščić, B. F. Woodfield, J. Chem. Thermodyn. 2018, 116,
- [28] a) O. Trofymluk, A. A. Levchenko, S. H. Tolbert, A. Navrotsky, Chem. Mater. 2005, 17, 3772-3783; b) A. Navrotsky, I. Petrovic, Y. Hu, C.-Y. Chen, M. E. Davis, Micropor. Mater. 1995, 4, 95-98.
- [29] J. D. Dunitz, J. Bernstein, Acc. Chem. Res. 1995, 28, 193 200.
- [30] D.-K. Bučar, R. W. Lancaster, J. Bernstein, Angew. Chem. Int. Ed. 2015, 54, 6972-6993; Angew. Chem. 2015, 127, 7076-7098.
- [31] a) Y.-Q. Tian, S.-Y. Yao, D. Gu, K.-H. Cui, D.-W. Guo, G. Zhang, Z.-X. Chen, D.-Y. Zhao, Chem. Eur. J. 2010, 16, 1137-1141; b) S.-Y. Yao, Y.-Q. Tian, CrystEngComm 2010, 12, 697-699; c) Y.-Q. Tian, L. Xu, C.-X. Cai, J.-C. Wei, Y.-Z. Li, X.-Z. You, Eur. J. Inorg. Chem. 2004, 1039-1044.
- [32] With the obvious exception of the highly radioactive, short-lived copernicium: J.-M. Mewes, O. R. Smits, G. Kresse, P. Schwerdtfeger, Angew. Chem. Int. Ed. 2019, 58, 17964-17968; Angew. Chem. 2019, 131, 18132-
- [33] N. Masciocchi, G. A. Ardizzoia, S. Brenna, F. Castelli, S. Galli, A. Maspero, A. Sironi, Chem. Commun. 2003, 2018-2019.
- [34] a) A search of the Cambridge Structural Database (CSD version 5.40, Feb 2019 update) also reveals two Hg^{II} tetrazolate frameworks, and a pyrazolate: D.-S. Liu, Y. Sui, G.-M. Ye, H.-Y. Wang, J.-Q. Liu, W.-T. Chen, J. Solid State Chem. 2018, 263, 182-189; b) X. Jin, M. Shao, H. Huang, J.

7



- Wang, Y. Zhu, *Huaxue Tongbao (Chin. Chem. Bull.)* **1982**, 336–337, 368; c) N. Masciocchi, G. A. Ardizzoia, A. Maspero, G. LaMonica, A. Sironi, *Inorq. Chem.* **1999**, *38*, 3657–3664.
- [35] N. R. Rightmire, T. P. Hanusa, Dalton Trans. 2016, 45, 2352-2362.
- [36] J. F. Fernández-Bertrán, M. P. Hernández, E. Reguera, H. Yee-Madeira, J. Rodriguez, A. Paneque, J. C. Llopiz, J. Phys. Chem. Solids 2006, 67, 1612–1617
- [37] T. Friščić, C. Mottillo, H. M. Titi, Angew. Chem. Int. Ed. 2020, 59, 1018–1029; Angew. Chem. 2020, 131, 1030–1041.
- [38] L. Yang, D. R. Powell, R. P. Houser, *Dalton Trans.* **2007**, 955–964.
- [39] A. Okuniewski, D. Rosiak, J. Chojnacki, B. Becker, Polyhedron 2015, 90, 47–57.
- [40] D. Rosiak, A. Okuniewski, J. Chojnacki, *Polyhedron* **2018**, *146*, 35–41.
- [41] N. Masciocchi, F. Castelli, P. M. Forster, M. M. Tafoya, A. K. Cheetham, Inorg. Chem. 2003, 42, 6147 – 6152.
- [42] Q.-F. Yang, X.-B. Cui, J.-H. Yu, J. Lu, X.-Y. Yu, X. Zhang, J.-Q. Xu, Q. Hou, T.-G. Wang, CrystEngComm 2008, 10, 1531 – 1538.
- [43] K. J. Harris, A. Lupulescu, B. E. G. Lucier, L. Frydman, R. W. Schurko, J. Magn. Reson. 2012, 224, 38–47.
- [44] a) C. Mottillo, T. Friščić, Molecules 2017, 22, 144; b) K. Užarević, T. C. Wang, S.-Y. Moon, A. M. Fidelli, J. T. Hupp, O. K. Farha, T. Friščić, Chem. Commun. 2016, 52, 2133–2136.
- [45] I. Huskić, J.-C. Christopherson, K. Užarević, T. Friščić, Chem. Commun. 2016, 52, 5120-5123.
- [46] R. Dovesi, A. Erba, R. Orlando, C. M. Zicovich-Wilson, B. Civalleri, L. Maschio, M. Rérat, S. Casassa, J. Baima, S. Salustro, B. Kirtman, WIREs Comput. Mol. Sci. 2018, 8, e1360.
- [47] a) A. D. Becke, J. Chem. Phys. 1993, 98, 5648-5652; b) C. Lee, W. Yang, R. G. Parr, Phs. Rev. B 1988, 37, 785-789.
- [48] S. Grimme, J. Antony, S. Ehrlich, H. Krieg, J. Chem. Phys. 2010, 132, 154104.
- [49] I. A. Baburin, S. Leoni, G. Seifert, J. Phys. Chem. B 2008, 112, 9437 9443.
- [50] a) S.-Z. Hu, Z.-H. Zhou, B. E. Robertson, Z. Kristallogr. 2009, 224, 375 383; b) S. Alvarez, Dalton Trans. 2013, 42, 8617 8636.

- [51] a) Y.-C. Chen, J.-Y. Tung, T.-K. Liu, W.-J. Tsai, H.-Y. Lin, Y.-C. Chang, J.-H. Chen, *Dalton Trans.* 2018, 47, 14774–14784; b) M. Brookhart, M. L. H. Green, G. Parkin, *Proc. Natl. Acad. Sci. USA* 2007, 104, 6908–6914.
- [52] J. Kozelka, Noncovalent Forces (Ed. S. Scheiner), Springer International Publishing Switzerland 2015, 129–158.
- [53] a) Whereas agostic interactions have been first introduced for metals with empty d-orbitals, they have also been associated with metal cations with available p-orbitals onlly, such as Sn^{II} or Ag^I. For examples, see: K. Izod, W. McFarlane, B. V. Tyson, I. Carr, W. Clegg, R. W. Harrington, Organometallics 2006, 25, 1135–1143; b) A. Ilie, C. I. Raţ, S. Scheutzow, C. Kiske, K. Lux, T. M. Klapötke, C. Silvestru, K. Karaghiosoff, Inorg. Chem. 2011, 50, 2675–2684.
- [54] R. F. W. Bader, J. Phys. Chem. A 1998, 102, 7314-7323.
- [55] M. Lein, Coord. Chem. Rev. 2009, 253, 625-634.
- [56] a) O. Z. Yeşilel, G. Günay, C. Darcan, M. S. Soylu, S. Keskin, S. W. Ng, CrystEngComm 2012, 14, 2817 2825; b) C.-S. Liu, P.-Q. Chen, E.-C. Yang, J.-L. Tian, X.-H. Bu, Z.-M. Li, H.-W. Sun, Z. Lin, Inorg. Chem. 2006, 45, 5812 5821.
- [57] W. Yuan, T. Friščić, D. Apperley, S. L. James, Angew. Chem. Int. Ed. 2010, 49, 3916–3919; Angew. Chem. 2010, 122, 4008–4011.
- [58] Nature Chem. 2016, 8, 987, Editorial.
- [59] D.-K. Bučar, G. M. Day, I. Halasz, G. G. Z. Zhang, J. R. G. Sander, D. G. Reid, L. R. MacGillivray, M. J. Duer, W. Jones, *Chem. Sci.* 2013, 4, 4417 – 4425.
- [60] a) A. J. Clough, N. M. Orchanian, J. M. Skelton, A. J. Neer, S. A. Howard, C. A. Downes, L. F. J. Piper, A. Walsh, B. C. Melot, S. C. Marinescu, J. Am. Chem. Soc. 2019, 141, 16323–16330; b) L. Sun, M. G. Campbell, M. Dincă, Angew. Chem. Int. Ed. 2016, 55, 3566–3579; Angew. Chem. 2016, 128, 3628–3642; c) M. Sadakiyo, T. Yamada, H. Kitagawa, ChemPlusChem 2016, 81, 691–701.

Manuscript received: November 21, 2019

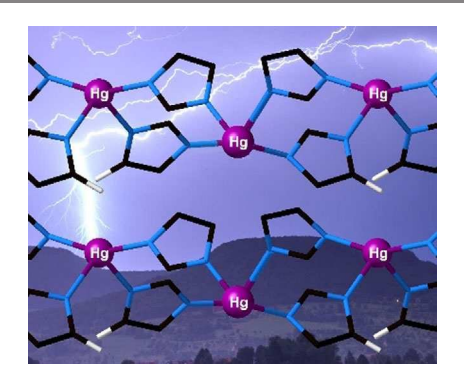
Accepted manuscript online: November 22, 2019

Version of record online: ■■ ■, 0000



FULL PAPER

Mechanochemical synthesis of mercury(II) imidazolate reveals a layered framework that is, based on reaction monitoring and theoretical calculations, more stable than the previously reported interpenetrated polymorph. The stabilization highlights a role for weak agostic contacts in MOF stability, whereas the inability to reproduce the previously known form represents the first example of the disappearing polymorph phenomenon in coordination chemistry.



Metal-Organic Frameworks

I. R. Speight, I. Huskić, M. Arhangelskis, H. M. Titi, R. S. Stein, T. P. Hanusa,* T. Friščić*



Disappearing Polymorphs in Metal– Organic Framework Chemistry: Unexpected Stabilization of a Layered Polymorph over an Interpenetrated Three-Dimensional Structure in Mercury Imidazolate